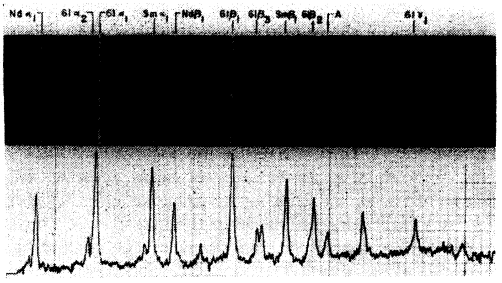

FIG. 1. The L spectrum of element Nos. 60, 61, and 62.

made to determine the dispersion curve for each chart. The dispersion of Bragg Angle per inch of chart was used. The Bragg Angle of each line of element 61 was determined from the dispersion curve for each chart. The reported value and limit of error are calculated from the average of the twelve individual measurements of each line.

A limit of error based on a 95 percent confidence level is reported instead of the usual probable error. Although the accuracy of this method is limited by the accuracy of the wave-length determination of the four standard lines, it is felt that this method is justified by its elimination of effects such as film shrinkage and has the advantage of an unbiased method of locating the apparent center of a line.

The wave-lengths determined in this laboratory are reported in Table I with wave-lengths previously reported for some of these lines.

Figure 1 is a photographic reproduction of the film showing the L spectra of element Numbers 60, 61, and 62 with a typical densitometer trace. The principal lines have been labeled. Although no attempt has been made to measure relative intensity of the lines, the apparent intensity may be seen from the densitometer tracing.

Weak lines presumed to be $61\beta_4$, $61\gamma_2$, $61\beta_7$, and $61\gamma_9$ were observed but no wave-length assignment was made due to low intensity and difficulty in determining the center of the line due to granularity of the film. A line marked (A) was observed at 1931.3±0.4 xu with an apparent intensity slightly less than the $61\gamma_1$ line which has not been satisfactorily identified. This corresponds to the wave-length of the $Nd\gamma_5$ line but it is doubtful that this is the origin due to its relatively high intensity. It is possible that this is an unresolved $K\alpha_1\alpha_2$ doublet of iron but this spectrograph has, in the past, resolved the $FeK\alpha_1\alpha_2$ doublet readily.

The authors wish to acknowledge the supervision and assistance of Dr. C. P. Keim, Superintendent, Isotope Development Department, in the performance of this work; also, the assistance of Dr. J. R. McNally, Isotope Physics Section, in the calculation of the wave-lengths of this element.

* This document is based on work performed for the AEC by Carbide and Carbon Chemicals Corporation at Oak Ridge, Tennessee.
[1] Burkhart, Peed, and Spitzer, Phys. Rev. **75**, 86 (1949).
[2] International Critical Tables **6**, 39 (1928).

Paramagnetic Anisotropy of Manganous Fluoride

J. W. STOUT AND MAURICE GRIFFEL*
Institute for the Study of Metals, University of Chicago, Chicago, Illinois
May 23, 1949

THE magnetic susceptibility of MnF_2, measured by Bizette and Tsai[1] and by de Haas, Schultz and Koolhaas[2] has a maximum at about 70°K. Stout and Adams[3] found an anomaly in the heat capacity with a maximum at 66.5°K. This behavior is typical of an antiferromagnetic substance in which the spins are presumably aligned by the exchange forces in an antiparallel fashion rather than parallel as in ferromagnetic substances.

We have measured the magnetic anisotropy of MnF_2 at temperatures from 12 to 300°K. Single crystals were grown from the melt in an atmosphere of HF. The crystals were oriented in a back reflection Laue camera. The anisotropy was determined by measuring the torque necessary to balance that exerted on the crystal by the homogeneous field of an electromagnet. MnF_2 is tetragonal, with the turile structure.[4] The crystals were mounted with the c-axis perpendicular to the axis of rotation of the crystal. Two samples were used. Crystal A, weighing 2.224 g, was a right circular cylinder cut with the c-axis parallel to the basal plane. Crystal B, weighing 0.2054 g, was an approximately square plate.

The results are illustrated in Figs. 1 and 2. Below 70°K the anisotropy becomes extraordinarily large. By combining our measurements with those on the powder susceptibilities, one can calculate $\chi_{\parallel}$ and $\chi_{\perp}$. Within the accuracy of the powder susceptibility data the susceptibility parallel to the c-axis approaches zero at the absolute zero of temperature. The perpendicular susceptibility increases by about 12 percent as the temperature drops from 70°K to 14°K. At 20°K $\chi_{\parallel}-\chi_{\perp}$ was measured over a range of fields from 2000 to 10,000 gauss. The maximum spread in values was 0.7 percent and there was no systematic variation with field strength.

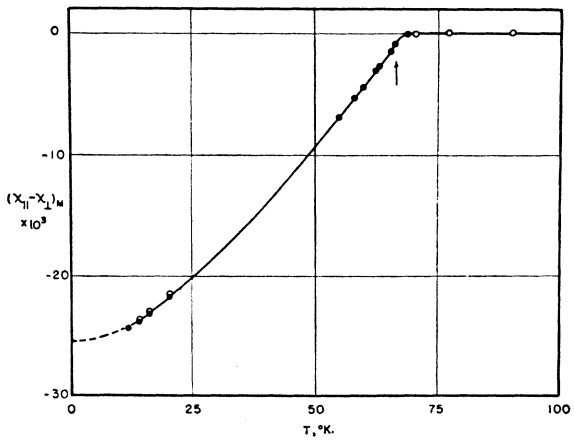

FIG. 1. Molal magnetic anisotropy of MnF_2. $\chi_{\parallel}$ and $\chi_{\perp}$ are molal susceptibilities parallel and perpendicular to the c-axis. Crystal A, open circles. Crystal B, filled circles. The arrow indicates the temperature of the heat capacity maximum.

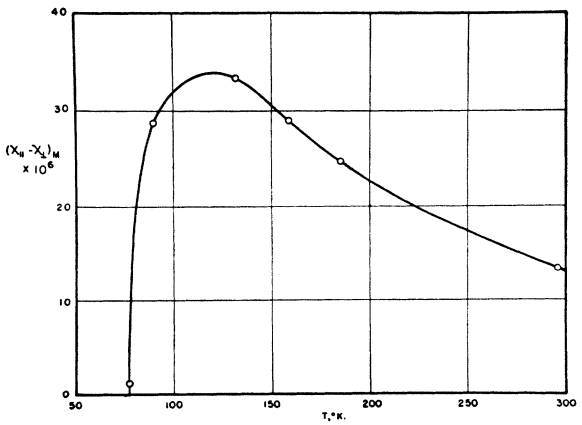

FIG. 2. Molal magnetic anisotropy of MnF_2. $\chi_{\parallel}$ and $\chi_{\perp}$ are molal susceptibilities parallel and perpendicular to the c-axis. Crystal A. Note that susceptibility scale is 1000 times that of Fig. 1.

Van Vleck[5] has proposed a theory of antiferromagnetism in which the exchange forces between neighboring atoms give rise to a Curie temperature and a maximum in the powder susceptibility. However, although the exchange forces align the spins with respect to one another, they cannot lead to an anisotropy since the energy is invariant under rotation with respect to the crystal axes.[6] The small anisotropy of MnF_2 observed at high temperatures is comparable to that observed in more dilute manganous salts,[7] which is explained by Van Vleck and Penney[8] as due to a slight splitting of the ^6S level of the free Mn^{++} ion by the crystalline electrostatic fields. In the case of MnF_2 the susceptibility parallel to the c-axis is the greater at high temperatures indicating that the alignment of spins parallel to this axis is energetically more stable by a few tenths of a wave number.

The cooperative phenomenon at temperatures below 70°K is is presumably due to the strong exchange coupling between the Mn^{++} ions. The deviation of the powder susceptibility at high temperatures from the free ion value is also caused by the exchange forces. The large anisotropy at temperatures below 70°K, where the spins are presumed cooperatively coupled antiparallel, occurs because the forces which at high temperatures can produce only a very small anisotropy become, when acting on a large group of coupled spins, energetically important compared to kT. These forces would serve to align the coupled spin system parallel to the c-axis and the anisotropy calculated from Van Vleck's theory of antiferromagnetism would then be in good qualitative agreement with our observations.

Magnetic dipole-dipole interactions could also, through a similar mechanism, produce an anisotropy. However, if the spins of the nearest neighboring Mn^{++} ions, which lie in chains parallel to the c-axis, are coupled antiparallel the dipole forces would favor an alignment of the spin system perpendicular to the c-axis.

A detailed account of this investigation will be published elsewhere.

* Atomic Energy Commission Fellow 1948–49.

[1] H. Bizette and B. Tsai, Comptes Rendus **209**, 205 (1939).
[2] de Haas, Schultz and Koolhaas, Physica **7**, 57 (1940).
[3] J. W. Stout and H. E. Adams, J. Am. Chem. Soc. **64**, 1535 (1942).
[4] Strukturbericht (Leipzig, 1931), Vol. I, p. 192.
[5] J. H. Van Vleck, J. Chem. Phys. **9**, 85 (1941).
[6] See J. H. Van Vleck, Phys. Rev. **52**, 1178 (1937).
[7] K. S. Krishnan and S. Banerjee, Trans. Roy. Soc. **A235**, 343 (1936).
[8] J. H. Van Vleck and W. G. Penney, Phil. Mag. **17**, 961 (1934).

An Accurate Nuclear Magnetic Resonance Method for Measuring Spin-Lattice Relaxation Times*

ERWIN L. HAHN
Physics Department, University of Illinois, Urbana, Illinois
May 23, 1949

THE bridge method[1] for obtaining nuclear magnetic resonance has been applied in conjunction with an electronic technique[2] which permits accurate measurements of spin-lattice relaxation times T_1. The recovery in time of a non-equilibrium value of the energetic component of nuclear magnetization, $M_z(t)$, toward thermal equilibrium M_0 is observed by measurement of resonance absorption and emission signal amplitudes on the oscilloscope which are proportional to $M_z(t)$. When an ensemble of spins, such as protons in H_2O, is subjected to a perturbing r-f field H_1 in a large d.c. magnetic field H_0 perpendicular to H_1, the excess population of spins n_0 in the ground state is reduced to a smaller value n_i. In general $n=N_{+\frac{1}{2}}-N_{-\frac{1}{2}}$ where $N_{+\frac{1}{2}}$ and $N_{-\frac{1}{2}}$ are the number of spins parallel and antiparallel to H_0 respectively, and n is proportional to $M_z(t)$. Upon removal of H_1 the recovery of n is given by

$$n=n_0[1+(n_i-n_0/n_0)e^{-t/T_1}].$$

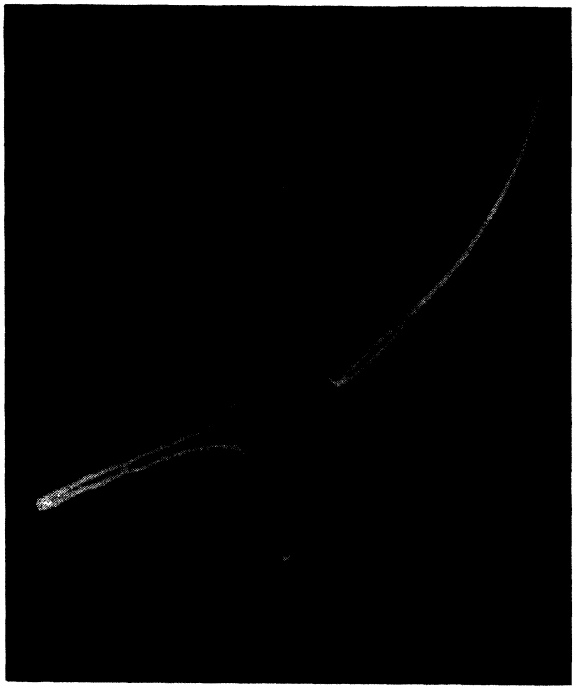

FIG. 1. The positive (n_0) and negative (n) signals represent slow passage resonance absorption and emission respectively. The emission signal occurs for $t=1/30$ sec. For t sufficiently large the n signal is positive, and coincides with the fixed n_0 absorption signal for t infinite.

A conventional Higginbotham array of scalar units provides interval timing between a single r-f pulse of large amplitude which inverts** M_0 to a negative value M_i (i.e. $N_{-\frac{1}{2}}>N_{+\frac{1}{2}}$ at $t=0$) and a later single r-f pulse, also of large amplitude, which inspects the amplitude and sign of M_z at a known time t. 30 c.p.s. modulation of the d.c. field H_0 is used to synchronize the interval times with passage through resonance, but no r-f field is applied to the sample between pulses. The operator arbitrarily initiates the first r-f square wave pulse which is adjusted to center automatically upon a resonance; the inspecting pulse, identical to the first one, automatically follows at a specified time t later. Combinations of scalar units are preset according to time intervals desired. In order to repeat data for a particular time interval, reset switches permit the process to be repeated. In order to inspect various points in time t on the exponential recovery of M_z toward thermal equilibrium, one needs simply to preset the proper

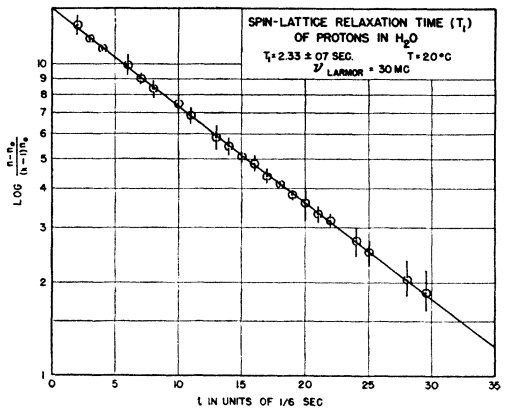

FIG. 2.